

# Frictional magnetodrag between spatially separated two-dimensional electron systems: Coulomb versus phonon mediated electron-electron interaction

Samvel M. Badalyan\* and Chang Sub Kim†

*Department of Physics, Chonnam National University, Kwangju 500-757, Korea*‡

(Dated: May 22, 2019)

## Abstract

We study the frictional drag due to Coulomb and phonon mediated electron-electron interaction in a double layer electron system exposed to a perpendicular magnetic field. Within the random phase approximation we calculate the dispersion relation of the intra Landau level magnetoplasmons at finite temperatures and distinguish their contribution to the magnetodrag. We calculate the transresistivity  $\rho_{Drag}$  as a function of magnetic field  $B$ , temperature  $T$ , and interlayer spacing  $\Lambda$  for a matched electron density. For  $\Lambda = 200$  nm we find that  $\rho_{Drag}$  is solely due to phonon exchange and shows no double-peak structure as a function of  $B$ . For  $\Lambda = 30$  nm,  $\rho_{Drag}$  shows the double-peak structure and is mainly due to Coulomb interaction. The value of  $\rho_{Drag}$  is about 0.3  $\Omega$  at  $T = 2$  K and for the half-filled second Lanadau level, which is about 13 times larger than the value for  $\Lambda = 200$  nm. At lower edge of the temperature interval from 0.1 to 8 K,  $\rho_{Drag}/T^2$  remains finite for  $\Lambda = 30$  nm while it tends to zero for  $\Lambda = 200$  nm. Near the upper edge of this interval,  $\rho_{Drag}$  for  $\Lambda = 30$  nm is approximately linear in  $T$  while for  $\Lambda = 200$  nm it decreases slowly in  $T$ . Therefore, the peak of  $\rho_{Drag}/T^2$  is very sharp for  $\Lambda = 200$  nm. This strikingly different magnetic field and temperature dependence of  $\rho_{Drag}$  ascribe we mainly to the weak screening effect at large interlayer separations.

---

\*Electronic address: badalyan@lx2.yerphi.am

†Electronic address: cskim@boltzmann.chonnam.ac.kr

‡Permanent address: Radiophysics Department, Yerevan State University, Yerevan, 375025 Armenia.

## I. INTRODUCTION

Frictional drag between two spatially separated two-dimensional (2D) electron systems is a powerful tool to probe electron-electron ( $e - e$ ) interaction and is of current intensive research interest both experimentally and theoretically [1, 2]. The drag effect manifests itself when a current with a density  $J_1$  driven along the layer 1 induces, via momentum transfer, an electric field  $E_2$  in the layer 2 under the condition that the layer 2 is an open circuit [3, 4].

Much experimental work was done in the magnetic field-free case to measure the drag effect in a coupled 2D and 3D electron system [5], between two 2D electron systems (2DES) [6, 7, 8, 9, 10, 11, 12], two 2D hole systems (2DHS) [13, 14], and also in a coupled 2DES-2DHS [13, 15]. Theoretical work on the frictional drag has been devoted to explain different momentum transfer mechanisms in a coupled 2DES-3DES [16, 17], 2DES-2DHS [18, 19, 20], 2DES-2DES [21, 22, 23, 24, 25, 26, 27, 28, 29, 30, 31, 32, 33], and recently in a 2DHS-2DHS [34]. Also, plasmon-enhancement of the drag due to many-body correlations at high temperatures has been studied theoretically [28, 30] and experimentally [9, 10]. Two possible interlayer  $e - e$  interaction mechanisms have been considered: One is the direct electrostatic Coulomb scattering and the other is the phonon-mediated effective interaction. The Coulomb drag calculations predict a  $T^2$  temperature dependence for the transresistivity  $\rho_{Drag}$  and a strong inter-layer spacing ( $\Lambda$ ) dependence as  $\Lambda^{-4}$  [23, 25]. However, the experimental results do not support the pure Coulomb mechanism [7, 8, 11]. The observed drag has a peak when the electron densities match,  $n_1 = n_2$ , and the scaled transresistivity,  $\rho_{Drag}/T^2$ , deviates from a constant value demonstrating a peak as a function of  $T$  well below Bloch-Grüneisen temperature. Also, the measured  $\rho_{Drag}$  for separations at least up to 50 nm exhibits almost no dependence on  $\Lambda$  and its value beyond  $\Lambda = 50$  nm is much bigger to be accounted for by Coulomb interaction alone. This led Gramila *et al.* [7] to propose an acoustical phonon-mediated scattering mechanism for the drag. This mechanism was studied extensively in Refs. 23, 24, 32, 33. The theoretical results are satisfactory to explain the main experimental findings. The phonon-mediated drag due to the bare electron-phonon ( $e - p$ ) coupling diverges when the transferred energy,  $\hbar\omega$ , from the layer 1 to the layer 2 is close to  $\hbar s q$  ( $\vec{q}$  is the transferred in-plane momentum). This divergence is eliminated by taking into account other scattering mechanisms such as screening and/or the finite phonon mean free

path [32]. It is found that, despite the weak  $e - p$  coupling, the effective phonon-mediated  $e - e$  interaction remains strong and competes with the Coulomb interaction. In general,  $e - p$  scattering in 2DESs is qualitatively different between in the small angle scattering (SAS) temperature region,  $T \ll \hbar s k_F$ , and in the large angle scattering (LAS) temperature region,  $T \sim \hbar s k_F$ , where  $s$  is the speed of sound and  $k_F$  the Fermi wave vector [35, 36]. In the SAS region,  $\hbar\omega \lesssim T$  and this results in the power law dependence of  $\rho_{Drag} \propto T^6$ . On the other hand, in the LAS region,  $\hbar\omega \approx 2\hbar s k_F$  and  $\rho_{Drag}$  varies linearly in  $T$ . As a consequence,  $\rho_{Drag}/T^2$  has a peak at the crossover from the SAS to LAS temperature region at the peak temperature  $T_{peak} < \hbar s k_F$ . In the LAS temperature region the momentum transfer is most efficient when momenta of the emitted and absorbed phonons are determined by the same Fermi wave vector  $k_{1F} = k_{2F}$ , this results in the peaked transresistivity when  $n_1 = n_2$ . In the SAS region there is no cutoff related to  $k_F$  that  $\rho_{Drag}$  shows a monotonous behavior as a function of  $n_2$ .

The frictional drag has been also investigated in the presence of a perpendicular magnetic field. The drag rate has been measured experimentally in a coupled 2DES [9, 37, 38, 39, 40, 41, 42, 43], 2DHS [13] as well in a 2DES-2DHS [39]. Also, the response of composite fermions to large wave vector scattering has been studied through phonon magnetodrag measurements [44]. In addition, recent measurements reveal a new regime of the magnetodrag in a coupled 2DES at mismatched densities  $n_1 \neq n_2$  in which the polarity of the drag voltage is opposite that normally found for electron systems [42, 45]. Theoretical investigations were mostly carried out with incorporating the direct Coulomb mechanism [46, 47, 48, 49]. These calculations show reasonable agreement with the experiments [37, 38] that at low temperatures  $\rho_{Drag}$  demonstrates an analog of the Shubnikov-De Haas oscillations with amplitudes by two order of magnitude enhanced compared to the zero field drag signal. At the matched densities the measured magnetodrag has a double-peak structure in magnetic field in the inter-quantum Hall plateau regions [38, 42]. This observation is in agreement with the earlier calculations of the Coulomb magnetodrag by Bønsager *et al.* [46, 47] who predicted this behavior caused by the interplay of screening and Landau quantization. However, the calculations by Wu *et al.* [48] and the experiments by Hill *et al.* [37] show oscillations without the double peak structure. The critical test of the theory was performed in a recent experiment by Lok *et al.* [45], which confirms that the transresistivity does not show the predicted double peak structure for the spin split Landau levels and

the double-peak structure at higher filling factors is not caused by the screening effect [43]. Notice also, as against to the zero magnetic field case, the scaled transresistivity  $\rho_{Drag}/T^2$  due to the pure Coulomb mechanism shows a peaked temperature dependence in the finite magnetic fields [46, 47]. In addition, the Coulomb magnetodrag calculations [48, 49, 50] reveal new features associated with interlayer magnetoplasmons, that was observed also experimentally [9].

As we described in the previous paragraph, the phonon-mediated drag is the dominant mechanism in the zero magnetic field case in a coupled 2DES, except for very closely spaced layers [7, 8, 11, 13, 32, 33]. Further, it was reported recently that the effective phonon and the Coulomb contributions to drag were comparable in a coupled 2DHS even with closely spaced layers. The phonon-mediated drag effect has been also investigated experimentally in the finite magnetic fields [13, 39] where it was found also that the phonon contribution was prevalent in the coupled 2DES, 2DHS, and 2DES-2DHS with large barriers. Up to now, however, it is rare to find theoretical works on the frictional drag mediated by phonon exchange in a finite magnetic field. The exceptions are recent treatments of the phonon drag at the Landau level filling factor  $\nu = 1/2$  by Chern-Simons composite fermion theory [51, 52].

The aim of the present paper is to investigate the direct Coulomb and the effective phonon-mediated frictional drag in a coupled 2DES exposed to a perpendicular magnetic field theoretically. For this system we calculate the dispersion relation of the intra-Landau level magnetoplasmons by taking into account finite temperature and distinguish the magnetoplasmon contribution to the magnetodrag. We calculate  $\rho_{Drag}$  as a function of magnetic field  $B$ , temperature  $T$ , and interlayer spacing  $\Lambda$ , and determine the relative contributions of Coulomb versus phonon-mediated  $e - e$  interaction to magnetodrag

This paper is organized as follows. In the next Sec. II we describe briefly the theoretical method we use to calculate the transresistivity, which follows mainly to Refs. 32, 47. In Sec. III we present and discuss our calculations. Finally, the results are summarized and the conclusions are given in Sec. IV.

## II. THEORY

Our theoretical model consists of two parallel electron layers exposed to a perpendicular magnetic field in the  $z$ -direction, separated by a distance  $\Lambda$  from center to center, each having the electron densities  $n_1$  and  $n_2$  and the layer extensions  $d_1$  and  $d_2$ . The experimentally measured quantity is the transresistivity defined as  $\rho_{Drag} = E_2/J_1$ . The main theoretical framework to calculate  $\rho_{Drag}$  is the Fermi liquid theory where the interlayer  $e-e$  interaction is treated perturbatively. The expression for  $\rho_{Drag}$  can be derived by using the linearized Boltzmann equation [25] or the memory function formalisms starting from the Kubo formula [26, 27, 29, 32]. Direct calculations show that in our model the transresistivity is represented in the standard form

$$\rho_{Drag} = -\frac{\hbar^2}{2e^2 n_1 n_2 T} \frac{1}{A} \sum_{\vec{q}} q^2 \int_0^\infty \frac{d\omega}{2\pi} \frac{|W_{12}(q, \omega)|^2}{|\varepsilon(q, \omega)|^2} \times \frac{\text{Im}\chi_1(q, \omega)\text{Im}\chi_2(q, \omega)}{\sinh^2(\hbar\omega/2T)} \quad (1)$$

where  $A$  is the normalization area,  $W_{ij}(q, \omega) = \sum_{\Upsilon} W_{ij}^{\Upsilon}(q, \omega)$  the total unscreened interlayer interaction matrix element ( $i, j = 1, 2$  are the layer indices),  $\varepsilon(q, \omega)$  the screening function, and  $\chi_i(q, \omega)$  the irreducible intralayer electron polarization functions (the interlayer electron polarization is neglected). The index  $\Upsilon$  refers to the type of  $e-e$  interaction. We consider direct Coulomb ( $\Upsilon = C$ )  $e-e$  interaction and effective  $e-e$  interaction, mediated by the exchange of piezoelectric ( $\Upsilon = PA$ ) and deformation ( $\Upsilon = DA$ ) acoustical phonons as well as the exchange of polar optical phonons ( $\Upsilon = PO$ ). Phonon mediated  $e-e$  interaction appears in second order perturbation theory with respect to the bare  $e-p$  coupling. The unscreened interaction matrix element of this process is visualized by the diagram in Fig. 1. The free phonon propagator

$$D^{\Upsilon}(Q, \omega) = 2\omega_Q^{\Upsilon} \hbar^{-1} \left[ \left( \omega + \frac{i}{2\tau_Q^{\Upsilon}} \right)^2 - (\omega_Q^{\Upsilon})^2 \right]^{-1} \quad (2)$$

with  $\vec{Q} = (\vec{q}, q_z)$ ,  $\omega_Q^{PA, DA} = sQ$  and  $\omega_Q^{PO} = \omega_{PO}$ , and a summation over phonon momenta corresponds to the internal phonon line (the dashed line in the diagram).  $\tau_Q^{\Upsilon}$  is the lifetime of the phonons. The vertex part of this diagram (the solid dots in Fig. 1) corresponds to

$$\Gamma_i^{\Upsilon} = \sqrt{B^{\Upsilon}(Q)} I_i(q_z d) \quad (3)$$

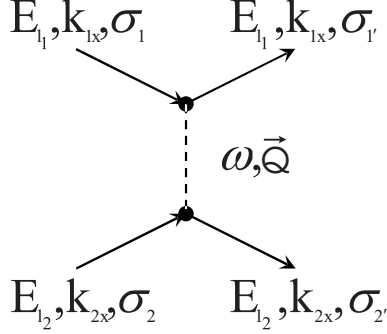


FIG. 1: Diagram for the effective phonon mediated  $e - e$  interaction. Here  $E_l$ ,  $k_x$ , and  $\sigma$  are the electron energy, the momentum in the Landau gauge, and the spin, respectively.

where  $B^Y(Q)$  are the bare  $e - p$  coupling functions [53] and  $I_i(\xi) = \int dz \rho_i(z) e^{i\xi z/d}$  are the form factors in  $z$ -direction (the remaining in-plane part of the form factor enters the definition of  $\chi(q, \omega)$ ). We assume that electron scattering takes place in the lowest electron subbands of infinitely high quantum wells with widths  $d_1 = d_2 = d$  and the subband density functions  $\rho_2(z) = \rho_1(z + \Lambda)$  in both layers do not depend on the subband index. In GaAs the PA interaction matrix element is given by the effective piezoelectric modulus which depends only on the polarization of the phonon and its direction of propagation. Since in this description of frictional drag we are interested in the average relaxation characteristics of the system, the anisotropy of PA interaction can be ignored. We describe PA interaction within the scope of the isotropic model [53] that leads to a scalar PA interaction constant. We assume also that all elastic parameters of the sample are the same and phonons are not reflected from the interfaces separating different materials (for instance between GaAs and AlGaAs).

Taking the summation over  $q_z$  and including also the Coulomb contribution, we obtain for the total unscreened interlayer  $e - e$  interaction matrix elements

$$\begin{aligned}
 W_{ij}(q, \omega) = & \frac{2\pi e^2}{\kappa_0} \frac{1}{q} \left\{ F_{ij}(qd) + \frac{\bar{\tau}_C}{\bar{\tau}_{PO}} \frac{\omega_{PO}^2}{\omega_{PO}^2 - \omega^2} F_{ij}(qd) \right. \\
 & + \frac{\bar{\tau}_C}{\bar{\tau}_{PA}} \frac{q}{\alpha} F_{ij}(\alpha d) \\
 & \left. + \frac{\bar{\tau}_C}{\bar{\tau}_{DA}} \left( F_3 \delta_{ij} + \frac{\omega^2}{2(s p_{PO})^2} \frac{q}{\alpha} F_{ij}(\alpha d) \right) \right\}
 \end{aligned} \quad (4)$$

where  $\kappa_0 = 13.1$  [54] is the GaAs static dielectric constant,  $\hbar p_{PO} = \sqrt{2m\hbar\omega_{PO}}$ ,  $\omega_{PO}$  the polar optical phonon frequency, and  $\alpha = \sqrt{q^2 - (\frac{\omega}{s} + \frac{i}{2s\tau_q})^2}$ . In the limit of infinite phonon

lifetime  $\alpha = \sqrt{q_\perp^2 - \omega^2/s^2}$  if  $q_\perp^2 > \omega^2/s^2$  and  $\alpha = -i\sqrt{q_\perp^2 - \omega^2/s^2}$  if  $q_\perp^2 < \omega^2/s^2$  with the positive square root branch. The form factors  $F$  are given by

$$F_{ij}(\xi) = \begin{cases} e^{-\frac{\Lambda}{d}\xi} F_1(\xi), & \text{if } i \neq j \\ F_2(\xi), & \text{if } i = j, \end{cases}, \quad F_1(\xi) = I(\xi)I(-\xi),$$

$$F_2(\xi) = \int dz_1 dz_2 \rho(z_1) \rho(z_2) e^{i\xi \frac{|z_1 - z_2|}{d}}, \quad F_3 = d \int dz \rho^2(z). \quad (5)$$

The following nominal scattering times are introduced in Eq. (4)

$$\frac{1}{\bar{\tau}_C} = \frac{2\omega_{PO}}{p_{PO}a^*}, \quad \frac{1}{\bar{\tau}_{PA}} = \frac{B_0^{PA}p_{PO}}{2\pi\hbar^2s}, \quad B_0^{PA} = \frac{\hbar(e\beta)^2}{2\varrho s},$$

$$\frac{1}{\bar{\tau}_{PO}} = 2\alpha_F\omega_{PO}, \quad \frac{1}{\bar{\tau}_{DA}} = \frac{B_0^{DA}p_{PO}^3}{\pi\hbar^2s}, \quad B_0^{DA} = \frac{\hbar\Xi^2}{2\varrho s} \quad (6)$$

where  $\alpha_F$  is the Frölich interaction constant,  $\Xi$  and  $e\beta$  the deformation and piezoelectric phonon potential constants,  $\varrho$  the crystal mass density, and  $a^*$  the effective Bohr radius. For GaAs we have  $\bar{\tau}_C \approx 0.024$  ps and the numerical values  $\bar{\tau}_{PO} \approx 0.14$  ps,  $\bar{\tau}_{PA} \approx 8$  ps,  $\bar{\tau}_{DA} \approx 4$  ps take we from [53].

We are interested in the experimental situations when the Landau levels are fully resolved, accordingly the scale of  $\omega$  over which a 2DES responds to an external perturbation is given by the width of the Landau band. Therefore, when  $\omega \ll \omega_{PO}$ , the optical phonon propagator  $D^{PO}(q, \omega)$  is never on the mass surface, and only virtual optical phonons can contribute to the magnetodrag in this regime. The PO phonon mediated contribution to total interaction,  $W_{ij}^{PO}(q, \omega)$  (the second term in Eq. (4)), at  $\omega = 0$ , behaves like the Coulomb contribution,  $W_{ij}^C(q, \omega)$  (the first term in Eq. (4)). And, because of the small  $\bar{\tau}_C/\bar{\tau}_{PO}$  coupling, simply results in about 17% renormalization of  $W_{ij}^C(q, \omega)$ . From Eqs. (4) and (5) one can see that  $W_{12}^C(q, \omega)$  is large when  $q\Lambda \lesssim 1$ . In drag experiments  $\Lambda$  is larger than  $d$  so we have usually  $qd \ll 1$ . The PA and DA phonon contributions,  $W_{ij}^{PA,DA}(q, \omega)$  (the third and forth terms in Eq. (4)), behave like a delta function because of the small phonon couplings  $\bar{\tau}_C/\bar{\tau}_{PA} \approx 3 \cdot 10^{-3}$  and  $\bar{\tau}_C/\bar{\tau}_{DA} \approx 1.5 \cdot 10^{-3}$ :  $W_{ij}^{PA,DA}$  are negligible with respect to the Coulomb term  $W_{ij}^C(q, \omega)$  for all over  $\omega$  and  $q$  except the close neighborhood of  $\omega = sq$  where  $\alpha$  is very small and we have again  $\alpha d \ll 1$ . Thus, the zero-limit approximation of the form factors  $F$  is well justified for both Coulomb and phonon mediated  $e - e$  interaction and we take  $F_{1,2}(\xi) \approx F_{1,2}(0)$  in our numerical calculations.

In the random phase approximation the dielectric tensor is obtained from the solution of a matrix Dyson equation for the dynamically screened interlayer interaction [55] and has the

form  $\varepsilon_{ij}(q, \omega) = \delta_{ij} - W_{ij}(q, \omega)\chi_j(q, \omega)$  (assuming no summation by the repeating indices). The screening function  $\varepsilon(q, \omega)$  is the determinant of the dielectric tensor and is given by

$$\begin{aligned}\varepsilon(q, \omega) = & (1 - W_{11}(q, \omega)\chi_1(q, \omega))(1 - W_{22}(q, \omega)\chi_1(q, \omega)) \\ & - W_{12}^2(q, \omega)\chi_1(q, \omega)\chi_2(q, \omega)\end{aligned}\quad (7)$$

In this approximation  $\chi(q, \omega)$  is determined by the bubble diagrams with the exact vertex part. Bønsager *et al.* [47] have shown that when the Landau levels are clearly resolved, corrections to the vertex part are small. In the first approximation they can be neglected and  $\chi(q, \omega)$  is given by

$$\begin{aligned}\chi(q, \omega) = & \frac{1}{\pi\ell_B^2} \sum_{l,l'=0}^{\infty} Q_{ll'}^2 \left( \frac{q^2\ell_B^2}{2} \right) \int_0^{\infty} \frac{dE}{\pi} f_T(E - E_F) \\ & \times \text{Im}G_l^R(E) \left( G_{l'}^R(E + \hbar\omega) + G_{l'}^A(E - \hbar\omega) \right),\end{aligned}\quad (8)$$

$\ell_B$  is the magnetic length and  $f_T$  the Fermi distribution function determined by the chemical potential  $E_F$ . The bare vertex functions  $Q_{ll'}$  are given by the gauge invariant part of the in-plane form factor

$$Q_{ll'}(t) = (l!/l'!)^{1/2} e^{-t/2} t^{(l-l')} L_{l'}^{l-l'}(t), \text{ for } l \leq l' \quad (9)$$

where  $L_{l'}^{l-l'}(t)$  is the associated Laguerre polynomial. For  $l' > l$  one can exploit the symmetry relation  $Q_{ll'}(t) = (-1)^{l-l'} Q_{l'l}(t)$ . In Eq. (8)  $G_l^{R,A}(E)$  are the electron retarded and advanced Green functions dressed by electron-impurity ( $e - i$ ) interaction. We treat  $e - i$  scattering in the short-range impurity model [56] and use the Green functions obtained by Ando and Uemura [57] in the self-consistent Born approximation

$$G_l^{R,A}(E) = 2 \left[ E - E_l + \sqrt{(E - E_l)^2 - \Gamma_0^2} \right]^{-1}. \quad (10)$$

In this approximation the half-width  $\Gamma_0 = \sqrt{\frac{2}{\pi} \hbar \omega_B \frac{\hbar}{\tau}}$  of the Landau level  $E_l = (l + 1/2)\hbar\omega_B$  is independent of the Landau index  $l$  ( $\omega_B$  is the cyclotron frequency and  $\tau$  is the transport relaxation time that determines the current in the drive layer via the mobility  $\mu = e\tau/m^*$ ,  $m^*$  is the electron effective mass). The chemical potential  $E_F(n, B, T, \mu)$  in distribution functions is determined implicitly from the electron density

$$n = -\frac{1}{2\pi\ell_B^2} \sum_{l=0}^{\infty} \int_0^{\infty} \frac{dE}{\pi} f_T(E - E_F) \text{Im}G_l(E). \quad (11)$$

Here we use the Green functions obtained by Gerhardts [58] in the improved self-consistent Born approximation

$$G_l(E) = -i \frac{\sqrt{2\pi}}{\Gamma_0} \exp\left(-2 \frac{(E - E_l)^2}{\Gamma_0^2}\right) \times \left[1 + \text{Erf}\left(i\sqrt{2} \frac{E - E_l}{\Gamma_0}\right)\right] \quad (12)$$

which correspond to the Gaussian density of states without the unphysical edges of Landau bands.  $\text{Erf}(z)$  is the error function.

Thus, Eqs. (1) and (4-12) determine the transresistivity of the double layer 2DES exposed to a perpendicular magnetic field and coupled via direct Coulomb and effective phonon mediated  $e - e$  interaction. In this treatment the Landau levels acquire broadening due to  $e - i$  scattering and each broadened state has its weighted contribution to drag. The electron energy remains dispersionless and the distribution functions do not depend on the position of the Landau oscillator center. For this reason  $\rho_{\text{Drag}}$  does not depend on the gauge non-invariant electron momenta  $k$ , as it should be, but also after performing the summation over all  $k$ , no interference occurs in Eq. (1) between different Fourier components  $\vec{q}$  both of the Coulomb [59] and the  $e - p$  interaction potentials. It should be noticed also that only such non-trivial treatment of  $e - e$ ,  $e - p$ , and  $e - i$  scattering allows the existence of the intra-Landau band magnetoplasmons and  $e - p$  scattering processes with a finite energy transfer  $\hbar\omega \neq 0$ . This is especially important in the regime of  $T$ ,  $\Gamma_0 \ll \hbar\omega_B$  under the consideration here. Without impurity broadening of the Landau levels, the phonon mediated magnetodrag in this regime is only due to exchange of pure virtual phonons with  $\hbar\omega = 0$  and  $q \neq 0$ . But this contribution is small with respect to the Coulomb magnetodrag for all phonon modes. In contrast to this, for finite  $\hbar\omega$ , acoustical phonon mediated  $e - e$  interaction diverges in  $\omega = sq$ . This divergence enhances strongly the phonon contribution to magnetodrag and makes it dominant at large interlayer separations.

### III. RESULT AND DISCUSSION

Below we present our calculations of  $\rho_{\text{Drag}}$  as a function of  $B$ ,  $T$ , and  $\Lambda$  in a symmetric double layer quantum well system with a matched electron density  $n = 2.5 \cdot 10^{15} \text{ m}^{-2}$ . We neglect the spin splitting and assume that the Landau levels are fully resolved and the odd filling factors correspond to a half-filled Landau levels. The spin degeneracy results in an

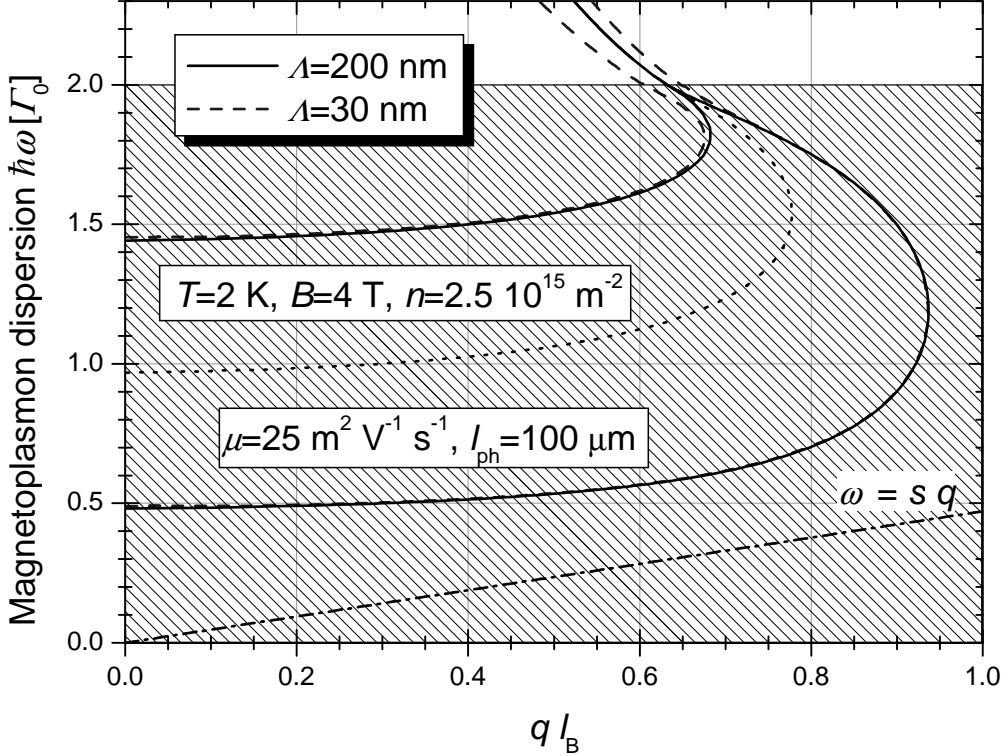


FIG. 2: Intra Landau level magnetoplasmon dispersion relation for the adopted parameters obtained from the zeros of the real part of the screening function. Dotted line shows zeros of the imaginary part of the screening function.

additional factor of 4 in Eq. (1). It is known that at temperatures below Bloch-Grüneisen temperature the frictional drag is dominated by the PA phonons in the case of  $B = 0$  [33], and the PO contribution is weak as we describe in the previous Section. Here we consider mainly PA phonon mediated  $e - e$  interaction. The inclusion of calculations for DA phonon mediated  $e - e$  interaction is straightforward. We take into account only the intra-Landau level magnetoplasmon modes and, in the low temperature regime ( $T \ll \omega_B$ ) under consideration here, we neglect the interlevel magnetoplasmon contributions to the magnetodrag. The intra-Landau level collective excitations [60] exist when a Landau level is partially filled. In Fig. 2 we plot the intra-Landau level magnetoplasmon dispersion relation obtained from the zeros of the real part of the screening function,  $\text{Re } \varepsilon(q, \omega(q)) = 0$ , with the imaginary part describing the damping. The spectra have two collective modes with the finite values  $\omega^-(0)$  and  $\omega^+(0)$  close to  $\Gamma_0/2$  and  $3\Gamma_0/2$  in the limit of  $q \rightarrow 0$ . When  $B$  varies in the second inter-plateau region from 3 to 4.5 T for  $T = 2$  K or  $T$  varies from 1 to 8 K for  $B = 4$  T,  $\omega^-(0)$  ( $\omega^+(0)$ ) is changed slightly, within 1% (5%).

The values of  $\omega^-(0)$  and  $\omega^+(0)$  increase monotonically in  $T$  in this temperature interval. In this magnetic field interval, they approach closely each other at  $B$  corresponding to the half-filled Landau level. The whole spectra are located in a finite range of  $q$  close to zero so that the magnetoplasmons have momenta  $q\ell_B < 1$  for the choice of parameters in Fig. 2. For such momenta the phonon energy  $\hbar sq$  (the dashed-dotted line in Fig. 2) lies below the magnetoplasmon energy near the lower edge of Landau band. Therefore, the phonon mediated  $e - e$  interaction effect on the magnetoplasmon spectrum is negligible. For energies  $\hbar\omega$  well below  $2\Gamma_0$  ( $\Gamma_0 \approx 6.5$  K,  $\Gamma_0/\hbar\omega_B \approx 0.08$  for  $B = 4$  T), both the splitting and broadening of each magnetoplasmon mode of the spectra are determined by the strong damping  $\text{Im } \chi(q, \omega(q))$ . The poles corresponding to these collective modes are moved into the complex  $\omega$ -plane and are located far from the real axis. Therefore, the two modes of the spectra are strongly mixed and damped and cannot be interpreted as the normal modes of the system. The imaginary part  $\text{Im } \varepsilon(q, \omega(q))$  has opposite sing to each other for these two collective modes. This corresponds to the situation when the energy from the magnetoplasmon with  $\text{Im } \varepsilon(q, \omega(q)) > 0$  is dissipated into the system and the energy is given to the magnetoplasmon with  $\text{Im } \varepsilon(q, \omega(q)) < 0$  by the system. Noticed that in this strongly dispersive system, the group velocity  $v_g \equiv d\omega(q)/dq$  shows anomalous behavior: It becomes infinite and changes its sign at certain points. This should not cause an alarm because in the regions of anomalous dispersion with  $\text{Re } \varepsilon(q, \omega(q)) = 0$ , the approximation  $\Delta\omega(q) \approx v_g q$  is not valid and the group velocity is not a useful concept [61]. Noticed also that the situation when the group velocity changes its sign in a finite wavenumber arises also, for instance, in the single particle spectra of magnetic edge states in 1D [62] and 2D [63, 64] electron systems exposed to a nonhomogeneous magnetic field. Towards the upper edge of the Landau band the damping decreases and becomes zero for  $\hbar\omega \geq 2\Gamma_0$ . Thus, in this model of the Landau band with sharp unphysical edges, the magnetoplasmons with energies  $\hbar\omega \geq 2\Gamma_0$  have no contribution to the magnetodrag. Near the upper edge of Landau band, the spectra are splitted into the symmetric and antisymmetric magnetoplasmon modes and this is due to the interlayer coupling, determined by the spacing  $\Lambda$ . One can see that for  $\Lambda = 30$  and 200 nm the magnetoplasmon dispersion shows different behavior in the close vicinity of  $\hbar\omega = 2\Gamma_0$ . In this region damping is vanishingly small, and the spectra describes long lifetime bound states of magnetoplasmons in a double layer system with a binding energy given by the splitting of the magnetoplasmon modes. For  $\Lambda = 30$  nm the

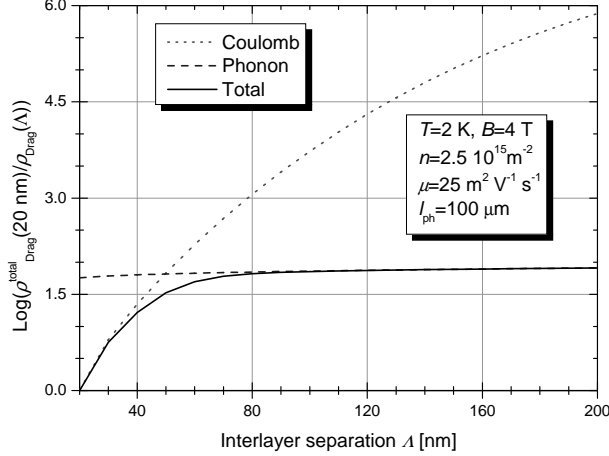


FIG. 3: Transresistivity as a function of the interlayer separation, normalized to the value of total transresistivity at  $\Lambda = 20$  nm. The contributions of the pure Coulomb and the pure phonon mediated couplings are shown together with their combined total contribution.

binding energy is about 1 K near the upper edge of the Landau band, and it decreases strongly with  $\Lambda$ . For  $\Lambda = 200$  nm Coulomb interlayer  $e - e$  interaction is obviously very weak, the binding energy is negligibly small, and the magnetoplasmon dispersion becomes degenerated. We note that the spectrum of inter Landau level magnetoplasmons near the upper edge of the Landau band has been calculated analytically for pure Coulomb  $e - e$  interaction by Khaetskii and Nazarov in Ref. 50, where the analogous dispersion curves for higher cyclotron harmonics was obtained.

In Fig. 3 we plot the transresistivity as a function of the interlayer spacing  $\Lambda$  for pure Coulomb  $e - e$  interaction,  $W_{ij}^C(q, \omega)$ , and for pure PA phonon mediated  $e - e$  interaction,  $W_{ij}^{PA}(q, \omega)$ . In addition, we plot the total  $\rho_{Drag}$  due to their combined effect,  $W_{ij}(q, \omega) = W_{ij}^C(q, \omega) + W_{ij}^{PA}(q, \omega)$ . In all three cases we calculate the screening function by taking  $W_{ij}(q, \omega) = W_{ij}^C(q, \omega) + W_{ij}^{PA}(q, \omega)$ . It is seen that the Coulomb mechanism dominates for  $\Lambda < 30$  nm with an approximately exponential decrease of  $\rho_{Drag}$  in  $\Lambda$  while the phonon mechanism dominates for  $\Lambda > 80$  nm with an approximately logarithmic decrease. They have comparable contributions to magnetodrag for the intermediate  $\Lambda$ , showing the equal contributions at about  $\Lambda = 50$  nm.

In Fig. 4 we plot the magnetic field dependence of total transresistivity due to Coulomb and PA phonon mediated  $e - e$  interaction. The transresistivity shows Shubnikov-De Haas oscillations as a function of  $B$  both for the  $\Lambda = 30$  and 200 nm spacings. For  $\Lambda = 200$  nm we

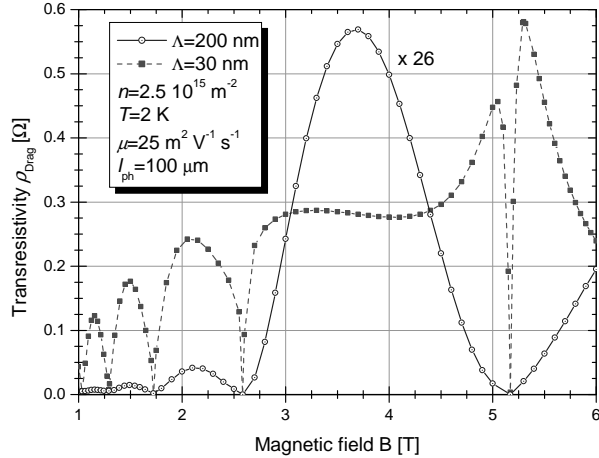


FIG. 4: Total transresistivity as a function of magnetic field plotted for the  $\Lambda = 30$  and  $200$  nm interlayer separations. The data for  $\Lambda = 200$  nm has been multiplied by a factor of 26.

find that  $\rho_{Drag}(B)$  has perfectly symmetric oscillations with strongly increasing amplitudes in  $B$ . We ascribe this to weak screening at large interlayer separations. For  $\Lambda = 30$  nm, in agreement with the calculations by Bønsager *et al.* [46] for pure Coulomb interaction,  $\rho_{Drag}(B)$  demonstrates a double peak structure around the filling factor  $\nu = 3$ , caused by strong screening. At low fields screening is relatively weak and, except for some asymmetry, no dip is visible for  $\nu \geq 4$ . However, screening has a flattening effect on the oscillation amplitudes in different inter-plateau regions for  $\Lambda = 30$  nm. The phonon contribution to the total magnetodrag for  $\Lambda = 30$  nm is about 5 to 10% in the second inter-plateau region, depending on  $B$ . For  $\Lambda = 200$  nm the Coulomb contribution to  $\rho_{Drag}(B)$  is negligible. It is seen from Fig. 4 that near  $\nu = 3$  the total  $\rho_{Drag}$  is about  $0.3 \Omega$  for  $T = 2$  K and  $\Lambda = 30$  nm, and this is approximately 13 times larger than  $\rho_{Drag}$  for  $\Lambda = 200$  nm. The magnitude of the calculated  $\rho_{Drag}$  and its strong decrease with increasing  $\Lambda$  are in good quantitative agreement with the experimental findings by Rubel *et al.* [39]. In this experiment, however, dips are also observed in the middle of Landau bands for samples with large interlayer separations. The lack of such dips in our calculations for  $\Lambda = 200$  nm might be an additional indication that these dips in the experiments should be attributed rather to the spin than the screening effect [9, 43, 45].

In Fig. 5 we present the temperature dependence of  $\rho_{Drag}$  and  $\rho_{Drag}/T^2$  for two different values of  $B$  and for  $\Lambda = 30$  and  $200$  nm in the temperature range from 0.1 up to 8 K. Although  $\rho_{Drag}/T^2$  shows a peaked temperature dependence for both  $\Lambda = 30$  and  $200$  nm,  $\rho_{Drag}$  demonstrates completely different behavior for  $\Lambda = 30$  and  $200$  nm as function of

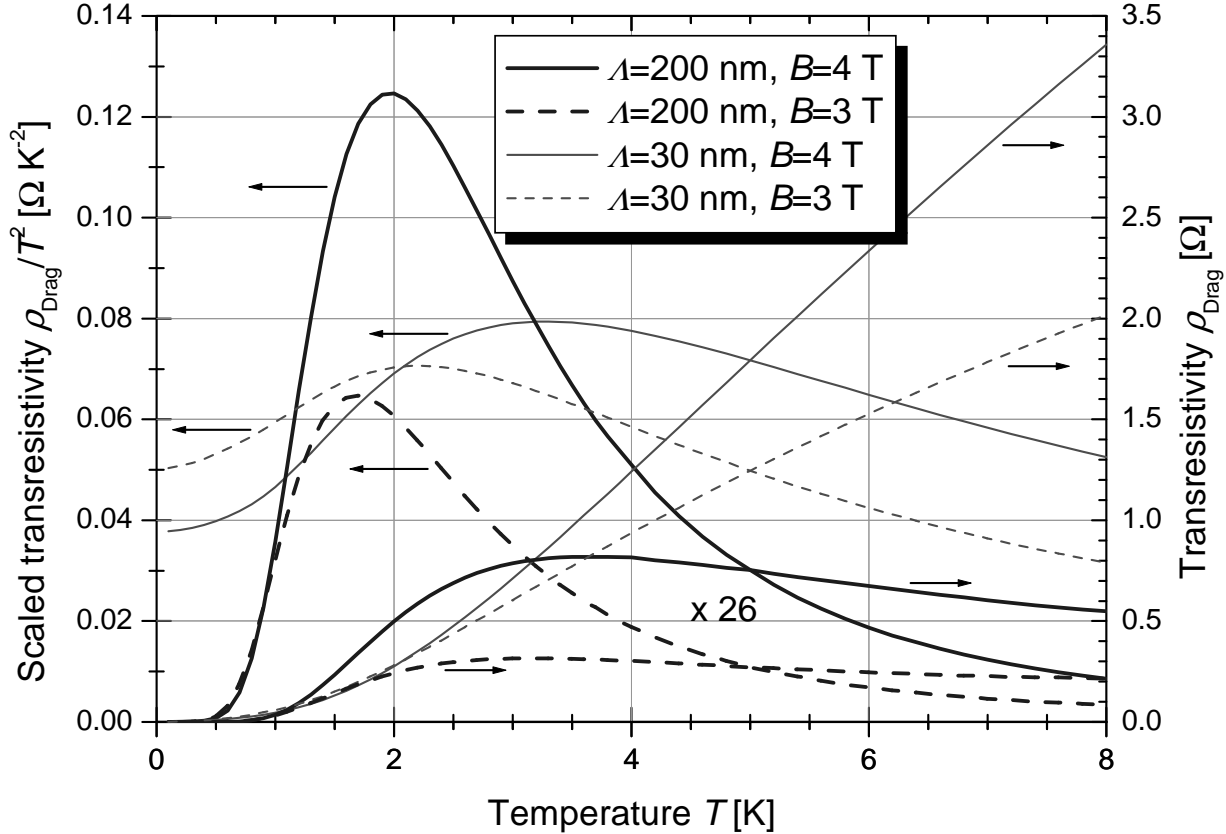


FIG. 5: Total transresistivity (the left axis) and scaled transresistivity (the right axis) versus temperature for  $B = 3$  and  $4$  T and for  $\Lambda = 30$  nm (thin lines) and  $200$  nm (thick lines). The data for  $\Lambda = 200$  nm has been multiplied by a factor of 26. The electron density is  $n = 2.5 \cdot 10^{15} \text{ m}^{-2}$ , the phonon mean free path  $l_{ph} = 100 \mu\text{m}$ , and the mobility  $\mu = 25 \text{ m}^{-2} \text{ V}^{-1} \text{ s}^{-1}$ .

$T$ . For  $\Lambda = 30$  nm the magnetodrag is mainly due to the Coulomb mechanism and is in agreement with the calculations by Bønsager *et al.* [46] for pure Coulomb interaction. At lower temperatures  $\rho_{Drag}$  has a subquadratic temperature dependence and  $\rho_{Drag}/T^2$  remains finite at low  $T$ . The transferred energy  $\hbar\omega$  is restricted by temperature,  $\hbar\omega \lesssim T$ , and the transferred momentum is, independently of  $\hbar\omega$ , restricted by the interlayer spacing,  $q \lesssim \Lambda^{-1}$  (in quantizing magnetic fields  $\Lambda^{-1}$  is always smaller than  $\ell_B^{-1}$ ). This is clearly seen in Fig. 6 where we plot the integrand over  $\hbar\omega$  in Eq. (1) for  $\Lambda = 30$  nm after taking the sum over  $\vec{q}$ . Even for relatively large  $T = 1$  K the integrand is strongly decreasing function of  $\omega$ . Therefore at low temperatures one can use the small  $\omega$  and the small  $q$  limit of the polarization function  $\chi(q, \omega)$ . In this limit both  $\text{Im } \chi(q, \omega)$  and  $\text{Im } \varepsilon(q, \omega)$  are linearly vanishing functions with  $\omega$  while  $\text{Re } \varepsilon(q, \omega)$  has a large maximum, determined by the electronic compressibility. By replacing the upper limit of the integration over  $\hbar\omega$  in

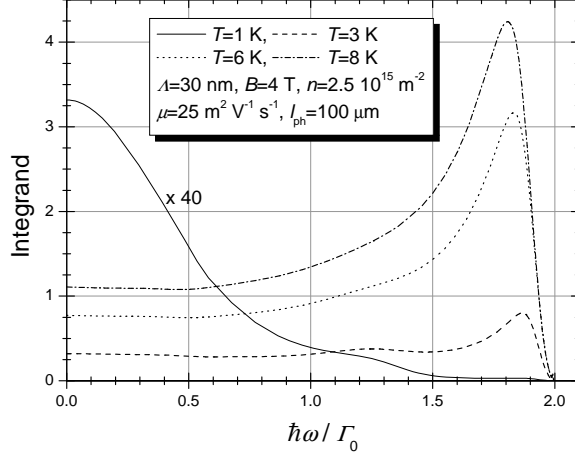


FIG. 6: Integrand over  $\omega$  in Eq. (1) after taking the sum over  $\vec{q}$  for  $\Lambda = 30$  nm and for different temperatures. The data for  $T = 1$  K has been multiplied by a factor of 40.

Eq. (1) with  $T$  and taking the static limit of the screening function out of the integration, one can obtain (cf. Fig. 5)

$$\rho_{Drag} \propto T^2 \int_0^T \frac{d\hbar\omega}{T} \frac{(\text{Im}\chi(\hbar\omega)/T)^2}{\sinh^2(\hbar\omega/2T)} \propto T^2. \quad (13)$$

At high temperatures all  $\hbar\omega < 2\Gamma_0$  contribute to the integral in Eq. (1). One can see from Fig. 6 that for  $T = 3, 6$ , and  $8$  K the integrand decreases very slowly in the region of small  $\omega$ . However, at energies close to  $\hbar\omega^-(0)$ , when the first magnetoplasmon mode is developed (cf. Fig. 2), the integrand starts to increase slowly. Further, at energies close to  $\hbar\omega^+(0)$ , when the second magnetoplasmon mode is developed (cf. Fig. 2), the integrand starts to increase strongly. The integrand reaches its well pronounced maximum, with an increasing height in  $T$ , just before it drops to zero at the upper edge of the Landau band  $\hbar\omega = 2\Gamma_0$ . This behavior of the integrand results in the peaked temperature dependence of  $\rho_{Drag}/T^2$  shown in Fig. 5 with an approximately linear temperature dependence of  $\rho_{Drag} \propto T$  at high temperatures, observed experimentally by Hill *et al.* [9].

The situation is completely changed for  $\Lambda = 200$  nm where the magnetodrag is mainly due to phonon exchange. At low temperatures  $\rho_{Drag}$  has stronger dependence on  $T$  than it has at the small interlayer separation. At high temperatures  $\rho_{Drag}$  decreases slowly with increasing  $T$ . This results in the very sharp peak of  $\rho_{Drag}/T^2$  as a function of  $T$  for  $\Lambda = 200$  nm (Fig. 5). This strikingly different behavior of  $\rho_{Drag}$  as a function of  $T$  for different  $\Lambda$  is a consequence of the fact that the main contribution to the phonon mediated drag comes from  $q \approx \omega/s$  for which effective unscreened  $e - e$  interaction diverges in the limit of infinite

phonon lifetime. Now the integrand over  $\omega$  in Eq. (1) is proportional to  $g_l(t) \equiv t (L_l(t))^2 e^{-t}$  with  $t = (\omega/s)^2 \ell_B^2/2$  and in the whole temperature range the main contribution to phonon magnetodrag makes  $t = t_l \sim 1$  ( $t_l$  are the zeros of the derivative of  $g_l(t)$ ), i.e. the finite  $\hbar\omega \approx \hbar s q \sim \hbar s / \ell_B \sim \Gamma_0$ . The small  $\omega$  and the small  $q$  approximation is not valid for  $\varepsilon(q, \omega)$  and it is rapidly decreasing function with  $\omega$  and the screening effect is weak in the phonon magnetodrag (cf. the curves corresponding to  $\Lambda = 30$  and  $200$  nm in Fig. 4). We obtain the following formula as an approximation to describe the temperature dependence of the transresistivity in this regime

$$\rho_{Drag} \sim \sum_l \frac{1}{\nu^2} \frac{t_l}{\vartheta} \frac{|W_{12}(t_l, y_l)|^2}{|\varepsilon(t_l, y_l)|^2} \frac{(\text{Im}\chi(t_l, y_l))^2}{\sinh^2(y_l/2\vartheta)} \quad (14)$$

where  $\vartheta \equiv T/\Gamma_0$  and  $y \equiv \hbar\omega/\Gamma_0$ . For  $B = 4$  T we have  $\nu = 2$  and the main contribution to the sum makes the outermost filled Landau level with  $l = 1$  and  $t_1 = 2 + \sqrt{3}$ . In GaAs  $2ms^2 \approx 0.23$  K and  $\Gamma_0 \approx 6.5$  K for  $\mu = 25$  m<sup>2</sup>V<sup>-1</sup>s<sup>-1</sup>, so we have  $t \approx (1.5y)^2$ . This gives  $\hbar\omega_1/2 \approx 4.2$  K as a crossover temperature of the temperature dependence of  $\rho_{Drag}(T)$ . At temperatures below  $\hbar\omega_1/2$ ,  $\sinh^2(\hbar\omega_1/2T)$  increases strongly with  $T$  and this determines mainly the behavior of  $\rho_{Drag}(T)$ . It is seen from Fig. 5 that for  $\Lambda = 200$  nm  $\rho_{Drag}/T^2$  tends to zero at low  $T$  in contrast to its finite value for  $\Lambda = 30$  nm. At temperatures above  $\hbar\omega_1/2$ ,  $\sinh^2(\hbar\omega_1/2T) \propto T^2$ , and the screening function  $\varepsilon(q_1, \omega_1)$  for such large arguments is small and increasing in  $T$ . This behavior together with the  $T^{-1}$  prefactor in Eq. (1) determines the temperature dependence of  $\rho_{Drag}$  at high  $T$ . One can see, however, from Fig. 5 that the actual peak position of  $\rho_{Drag}(T)$  is shifted to the left from  $\hbar\omega_1/2$ . For  $\Lambda = 200$  nm the integrand over  $\omega$  in Eq. (1) after taking the sum over  $\overrightarrow{q}$  manifests itself to three strongly pronounced peaks near  $y = 0.45$ ,  $1.25$ , and  $2$ , and their positions are relatively stable with respect to temperature (see Fig. 7). Notice, as against the situation of the Coulomb magnetodrag, even for small  $T = 1$  K the integrand is approximately zero in the region of small  $\omega$  and has strongly pronounced peak at large  $\omega$ . The main highest peak of the integrand near  $y = 1.25$ , as we already discussed, is related to the maximum of  $g_1(t)$  at  $t_1^+ = 2 + \sqrt{3}$  corresponding to  $y = y_1^+ = 1.29$ . The left small peak of the integrand near  $y = 0.45$  is related to another maximum of the function  $g_1(t)$  at  $t_1^- = 2 - \sqrt{3}$  ( $y_1^- = 0.35$ ) and also to the maximum of the function  $g_0(t)$  at  $t_0 = 1$  ( $y_0 = 0.67$ ). This second peak contribution to  $\rho_{Drag}(T)$  shifts the actual crossover temperature of  $\rho_{Drag}(T)$  to the left so that  $T_{peak} \approx 3.6$  K (Fig. 5). One can see, however, that the positions of the first two peaks of the integrand is not

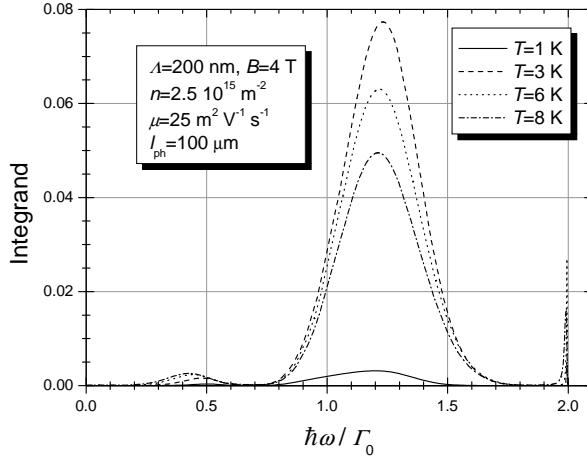


FIG. 7: Integrand over  $\omega$  in Eq. (1) after taking the sum over  $\vec{q}$  for  $\Lambda = 200$  nm and for different temperatures.

far from the magnetoplasmon energies  $\hbar\omega^\pm(0)$ . Therefore the magnetoplasmons contribute also to the formation of these peaks to some extend. Nevertheless, it is clear from the very weak dependence of the total  $\rho_{Drag}$  on  $\Lambda$  (Fig. 3) that the magnetoplasmon contribution to  $\rho_{Drag}$  for  $\Lambda = 200$  nm is a small correction to the phonon contribution. The third peak of the integrand in the very close vicinity of the upper edge of the Landau band is a pure magnetoplasmon effect (cf. Fig. 2 and Fig. 7). Immediately below the upper edge of Landau band the magnetoplasmon damping is very small and this results in the very sharp peak of the integrand with a relatively small contribution to  $\rho_{Drag}(T)$ . Thus, at high temperatures we obtain that for  $\Lambda = 200$  nm  $\rho_{Drag}$  decreases slowly with  $T$  (Fig. 5). This extraordinary temperature dependence of  $\rho_{Drag}$  is mainly due to the weak screening effect at large interlayer separations and the screening is weak because the phonons with large energies and momenta realize  $e - e$  interaction between remote layers. Notice that the  $T^{-1}$  dependence of  $\rho_{Drag}(T)$  for the pure Coulomb interlayer interaction in one of the typical scattering regions was also reported by Khaetskii and Nazarov [50]. As far as we know at present no magnetodrag measurements are available in the above regime and the experimental test of the temperature dependence of phonon magnetodrag is critical.

#### IV. SUMMARY AND CONCLUSIONS

We have calculated the transresistivity between spatially separated electron layers in a perpendicular magnetic fields. We take into account both direct electrostatic Coulomb and

effective phonon mediated  $e - e$  interaction. For this system we calculate the dispersion relation of the intra-Landau level magnetoplasmons within the random phase approximation at the finite temperatures and distinguish the magnetoplasmon contribution to the magnetodrag. We find the strikingly different magnetic field and temperature dependence of the transresistivity for the small and large interlayer separations. When  $\Lambda = 30$  nm, the transresistivity shows a slight dip as a function of  $B$  in the middle of the second spin-degenerated Landau band with the total  $\rho_{Drag}$  about  $0.3 \Omega$  (the phonon mean free path is  $100 \mu\text{m}$ , the mobility  $\mu = 25 \text{ m}^2 \text{ V}^{-1} \text{ s}^{-1}$ ,  $T = 2 \text{ K}$ , and  $n = 2.5 \cdot 10^{15} \text{ m}^{-2}$ ), which, depending on  $B$ , includes about 5 to 10% of the phonon contribution due to piezoelectric interaction. When  $\Lambda = 200$  nm, the Coulomb contribution to magnetodrag is negligible. And,  $\rho_{Drag}$  shows no dip and the total drag around filling factor  $\nu = 3$  is about 13 times less than the value for  $\Lambda = 30$  nm. This is in good agreement with the experimental findings by Rubel *et al.* [39]. The scaled transresistivity  $\rho_{Drag}/T^2$  has a peaked temperature dependence for both  $\Lambda = 30$  and 200 nm. At low  $T$ ,  $\rho_{Drag}/T^2$  remains finite for  $\Lambda = 30$  nm, while for  $\Lambda = 200$  nm it tends to zero. At high  $T$ ,  $\rho_{Drag}$  is approximately linear in  $T$  for  $\Lambda = 30$  nm while for  $\Lambda = 200$  nm it decreases slowly with  $T$ . Therefore, the peak of  $\rho_{Drag}/T^2$  as function of  $T$  is very sharp for the large separation  $\Lambda = 200$  nm. We ascribe this to the weak screening effect at large interlayer separations where the phonon mechanism dominates with the large transferred energy and momentum.

### Acknowledgments

This work was supported by Chonnam National University under a grant in the year of 2002. We are grateful to R. Gerhardts, W. Dietsche, and K. von Klitzing for useful discussions. SMB acknowledges the support and hospitality in Max-Planck-Institute for Solid State Researches where this work was initiated.

---

[1] J. P. Eisenstein, in *Perspectives in Quantum Hall Effects: Novel Quantum Liquids in Low-Dimensional Semiconductor Structures*, edited by S. Das Sarma and A. Pinczuk (Wiley, New-York, 1997).

[2] A. Rojo, J. Phys.: Condens. Matter **11**, R31 (1999).

- [3] M. B. Pogrebinskii, Sov. Phys. Semicond. **11**, 372 (1977).
- [4] P. J. Price, Physica **117 & 118**, 750 (1983).
- [5] P. M. Solomon, P. J. Price, D. J. Franck, and D. C. La Tulipe, Phys. Rev. Lett. **63**, 2508 (1989).
- [6] T. J. Gramila, J. P. Eisenstein, A. H. MacDonald, L. N. Pfeiffer, and K. W. West, Phys. Rev. Lett. **66**, 1216 (1991).
- [7] T. J. Gramila, J. P. Eisenstein, A. H. MacDonald, L. N. Pfeiffer, and K. W. West, Phys. Rev. B **47**, 12 957 (1993).
- [8] H. Rubel, E. H. Linfield, D. A. Ritchie, K. M. Brown, M. Pepper, and G. A. C. Jones, Semicond. Sci. Technol. **10**, 1229 (1995).
- [9] N. P. R. Hill, J. T. Nicholls, E. H. Linfield, M. Pepper, D. A. Ritchie, G. A. C. Jones, B. Y.-K. Hu, and K. Flensberg, Phys. Rev. Lett. **78**, 2204 (1997).
- [10] H. Noh, S. Zelakiewicz, X. G. Feng, T. J. Gramila, L. N. Pfeiffer, and K. W. West, Phys. Rev. B **58**, 12 621 (1998).
- [11] H. Noh, S. Zelakiewicz, T. J. Gramila, L. N. Pfeiffer, and K. W. West, Phys. Rev. B **59**, 13 114 (1999).
- [12] M. Kellogg, J. P. Eisenstein, L. N. Pfeiffer, and K. W. West, preprint archived at cond-mat/0206547.
- [13] C. Jörger, S. J. Cheng, H. Rubel, W. Dietsche, R. Gerhardts, P. Sprecht, K. Eberl, and K. von Klitzing, Phys. Rev. B **62**, 1572 (2000).
- [14] R. Phyllarisetty, H. Noh, D. C. Tsui, E. P. De Poortere, E. Tutuc, and M. Shayegan, Phys. Rev. Lett. **89**, 016805 (2002).
- [15] U. Sivan, P. M. Solomon, and H. Shtrikman, Phys. Rev. Lett. **68**, 1196 (1992).
- [16] B. Laikhtman and P. M. Solomon, Phys. Rev. B **41**, 9921 (1990).
- [17] I. I. Boiko, P. Vasilopoulos, and Yu. Sirenko, Phys. Rev. B **45**, 13 538 (1992).
- [18] H. C. Tso, P. Vasilopoulos, and F. M. Peeters, Phys. Rev. Lett. **70**, 2146 (1993).
- [19] Świerkowski, J. Szymański, and Z. W. Gortel, Phys. Rev. Lett. **74**, 3245 (1995)
- [20] G. Vignale and A. H. MacDonald, Phys. Rev. Lett. **76**, 2786 (1996).
- [21] I. I. Boiko and Yu. Sirenko, Phys. Status Solidi B **159**, 805 (1990).
- [22] D. L. Maslov, Phys. Rev. B **45**, 1911 (1992).
- [23] H. C. Tso, P. Vasilopoulos, and F. M. Peeters, Phys. Rev. Lett. **68**, 2516 (1992).

- [24] C. Zhang and Y. Takahashi, *J. Phys.: Condens. Matter* **5**, 5009 (1993).
- [25] A.-P. Jauho and H. Smith, *Phys. Rev. B* **47**, 4420 (1993).
- [26] L. Zheng and A. H. MacDonald, *Phys. Rev. B* **48**, 8203 (1993).
- [27] A. Kamenev and Y. Oreg, *Phys. Rev. B* **52**, 7516 (1995).
- [28] K. Flensberg and B. Y.-K. Hu, *Phys. Rev. Lett.* **73**, 3572 (1994).
- [29] K. Flensberg, B. Y.-K. Hu, A.-P. Jauho, and J. Kinaret, *Phys. Rev. B* **52**, 14 761 (1995).
- [30] K. Flensberg and B. Y.-K. Hu, *Phys. Rev. B* **52**, 14 796 (1995).
- [31] Świerkowski, J. Szymański, and Z. W. Gortel, *Phys. Rev. B* **55**, 2280 (1997).
- [32] M. C. Bønsager, K. Flensberg, B. Y. Hu, and A. H. MacDonald, *Phys. Rev. B* **57**, 7085 (1998).
- [33] S. M. Badalyan and U. Roessler, *Phys. Rev. B* **59**, 5643 (1999).
- [34] E. H. Hwang, S. Das Sarma, V. Braude, and A. Stern, preprint archived at cond-mat/0202249.
- [35] V. Karpus, *Sov. Phys. Semicond.* **20**, 6 (1986); **22**, 268 (1988).
- [36] S. M. Badalyan and Y. B. Levinson, *Sov. Phys. Solid State* **30**, 1592 (1988); S. M. Badalyan *Sov. Phys. Semicond.* **3**, 1087 (1989).
- [37] N. P. R. Hill, J. T. Nicholls, E. H. Linfield, M. Pepper, D. A. Ritchie, A. R. Hamilton, and G. A. C. Jones, *J. Phys. Condens. Matt.* **8**, L557 (1996).
- [38] H. Rubel, A. Fischer, W. Dietsche, K. von Klitzing, and K. Eberl, *Phys. Rev. Lett.* **78**, 1763 (1997).
- [39] H. Rubel, A. Fischer, W. Dietsche, C. Joerger, K. von Klitzing, and K. Eberl, *Physica E* **1**, 160 (1997).
- [40] N. K. Patel, E. H. Linfield, K. M. Brown, M. Pepper, D. A. Ritchie, and G. A. C. Jones, *Semicond. Sci. Technol.* **12**, 309 (1997).
- [41] M. P. Lilly, J. P. Eisenstein, L. Pfeiffer, and K. W. West, *Phys. Rev. Lett.* **80**, 1714 (1998).
- [42] X. G. Feng, S. Zelakiewicz, H. Noh, T. J. Gramila, L. N. Pfeiffer, and K. W. West, *Phys. Rev. Lett.* **81**, 3219 (1998).
- [43] C. Jörger, W. Dietsche, W. Wegscheider, and K. von Klitzing, *Physica E* **6**, 586 (2000).
- [44] S. Zelakiewicz, H. Noh, T. J. Gramila, L. N. Pfeiffer, and K. W. West, *Phys. Rev. Lett.* **85**, 1942 (2000).
- [45] J. G. S. Lok, S. Kraus, M. Pohlt, W. Dietsche, K. von Klitzing, W. Wegscheider, and M. Bichler, *Phys. Rev. B* **63**, (2001).
- [46] M. C. Bønsager, K. Flensberg, B. Y.-K. Hu, and A.-P. Jauho, *Phys. Rev. Lett.* **77**, 1366

(1996).

- [47] M. C. Bønsager, K. Flensberg, B. Y.-K. Hu, and A.-P. Jauho, Phys. Rev. B **56**, 10314 (1997).
- [48] M. W. Wu, H. L. Cui, and N. J. M. Horing, Modern Phys. Lett. B **7**, 279, (1996).
- [49] A. Manolescu and B. Tanatar, Physica E **13**, 80 (2002).
- [50] A. V. Khaetskii and Yuli V. Nazarov, Phys. Rev. B **59**, 7551 (1999).
- [51] D. V. Khveshchenko, Phys. Rev. B **61**, 7227 (2000).
- [52] M. C. Bønsager, Y. B. Kim, and A. H. MacDonald, Phys. Rev. B **62**, 10 949 (2000).
- [53] V. F. Gantmakher and Y. B. Levinson, *Scattering of Carriers in Metals and Semiconductors* (North-Holland, Amsterdam, 1987).
- [54] S. Adachi, J. Appl. Phys. **58**, R1 (1985).
- [55] S. Das Sarma and A. Madhukar, Phys. Rev. B **23**, 805 (1981).
- [56] T. Ando, A. Fowler, F. Stern, Rev. Mod. Phys. **54**, 437 (1982).
- [57] T. Ando and Y. Uemura, J. Phys. Soc. Jpn. **36**, 959 (1974).
- [58] R. Gerhardts, Z. Phys. B **21**, 275 (1975); **21** 285 (1975).
- [59] S. M. Badalian, U. Rössler, and M. Potemski, J. Phys.: Condensed Matter **5**, 6719 (1993).
- [60] D. Antoniou, A. H. MacDonald, and J. C. Swihart, Phys. Rev. B **41**, 5440 (1990).
- [61] J. D. Jackson, *Classical Electrodynamics* (John Wiley & Sons Inc., USA, 1975).
- [62] S. M. Badalyan and F. M. Peeters, Phys. Rev. B **64**, 155303 (2001).
- [63] F. M. Peeters and A. Matulis, Phys. Rev. B **48**, 15166 (1993).
- [64] F. M. Peeters, J. Reijnders, S. M. Badalyan, and P. Vasilopoulos, Microelectron. Eng. **74**, 405 (1999).